DOI: 10.1002/cplu.201200257

Coupling of Azomethine Ylides with Nitrilium Derivatives of *closo*-Decaborate Clusters: A Synthetic and Theoretical Study

Aleksey L. Mindich,[a] Nadezhda A. Bokach,*[a] Maxim L. Kuznetsov,[b] Matti Haukka,[c] Andrey P. Zhdanov,[d] Konstantin Yu. Zhizhin,[d] Serguei A. Miltsov,[a] Nikolay T. Kuznetsov,[d] and Vadim Yu. Kukushkin*[a, e]

The azomethine ylides *p*-$R^3C_5H_4N^+CH^-COC_6H_4R^2$-*p* (**3a**: R^3=H, R^2=H, X=Br; **3b**: R^3=H, R^2=Me, X=I; **3c**: R^3=H, R^2=OMe, X=I; **3d**: R^3=H, R^2=F, X=I; **3e**: R^3=Me, R^2=Me, X=Br) react with the nitrile functionality of the *closo*-decaborate clusters $[Bu^n{}_4N][B_{10}H_9(NCR^1)]$ (**1a**: R^1=Me; **1b**: R^1=Et; **1c**: R^1=Ph) in a CH_3NO_2 solution under mild conditions (20–25 °C, 2 min) to afford selectively products of the nucleophilic addition (ca. quantitative yields based on NMR analysis in [D$_6$]DMSO, 71–87% yield of isolated products). These products are the borylated enamino ketones as the salts bearing exclusively a tetrabutylammonium cation $[Bu^n{}_4N][B_{10}H_9\{NCR^1{=}C(N^+C_5H_4R^3\text{-}p)COC_6H_4R^2\text{-}p\}]$ (**4a–h,k–n**) or the mixed salts $[Bu^n{}_4N]_{1-x}[p\text{-}R^3C_5H_4N^+CH_2COC_6H_4R^2\text{-}p]_x[B_{10}H_9\{NCR^1{=}C(N^+C_5H_4R^3\text{-}p)COC_6H_4R^2\text{-}p\}]$ (**4i**, **4j**, and **4o**). This reaction represents the first example of the selective nucleophilic addition of pyridinium azomethine ylides to the nitrile group and the first example of new C–C bond formation in the reaction of nitrilium derivatives of boron clusters with any nucleophiles so far tested. Compounds **4a–h,k–n** were characterized by ICP-MS, high resolution ESI-MS, molar conductivity, and IR, ^{1}H, ^{13}C{^{1}H}, and ^{11}B{^{1}H} NMR spectroscopy. The structures of **4a** and **4b** were determined by a single-crystal X-ray analysis. Theoretical calculations at the DFT level allowed the interpretation of the observed reaction selectivity, which is driven mostly by thermodynamic rather than kinetic factors, and steric repulsion between the boron cluster and the azomethine ylide molecule plays a crucial role. The activation of the nitrile group upon binding to the boron cluster is explained in terms of the electrostatic arguments. The mechanisms of the nucleophilic addition and the hypothetical cycloaddition between the azomethine ylide and nitriles were investigated in detail.

Introduction

In the past decade, various polyhedral boranes were the subject of significant attention, first of all, because of their various useful properties and important applications such as, for example in boron neutron-capture cancer therapy.[1] Although some reactions leading to functionalization of boron clusters are known,[2,3] the reactivity of the borylated C≡N functionality still remains scarcely investigated. However, the data for various borylated nitrilium species gradually emerging in the literature disclose a high reactivity of the C≡N group that is subject to facile additions of H_2O,[4–6] R′OH,[7–9] or amines[7,8,10] thus providing an easy route for the functionalization.

Previously[11] our research group observed that the C≡N moiety bound to the *closo*-decaborate cluster unit is so reactive toward 1,3-dipolar cycloaddition (DCA) of acyclic *Z*-nitrones, that the cycloaddition (CA) of these dipoles proceeds rapidly and under mild conditions furnishing substituted 2,3-dihydro-1,2,4-oxadiazoles. Following this study,[11] and in the framework of our ongoing project on 1,3-dipolar cycloaddition to the C≡N group in nitriles (for reviews see Ref. [12–15] and for recent studies see Ref. [16–20]) and isocyanides (for a review see Ref. [12] and for a recent study see Ref. [21]) we attempted CA between nitrilium decaborates and azomethine ylides (see Scheme 3 later) having an initial aim to generate novel imidazolinium systems that functionalizes the *closo*-decaborate cluster unit.

[a] A. L. Mindich, N. A. Bokach, S. A. Miltsov, V. Y. Kukushkin
Department of Chemistry, Saint Petersburg State University
Universitetsky Pr. 26, 198504 Stary Petergof (Russian Federation)
Fax: (+7) 812-4286939
E-mail: bokach@nb17701.spb.edu
kukushkin@vk2100.spb.edu

[b] M. L. Kuznetsov
Centro de Química Estrutural, Complexo I, Instituto Superior Técnico
Universidade Técnica de Lisboa
Avenida Rovisco Pais, 1049-001 Lisbon (Portugal)

[c] M. Haukka
Department of Chemistry, University of Jyväskylä
P.O. Box 35, 40014 University of Jyväskylä (Finland)

[d] A. P. Zhdanov, K. Y. Zhizhin, N. T. Kuznetsov
N. S. Kurnakov Institute of General and Inorganic Chemistry
Russian Academy of Sciences
31 Leninsky Pr., 119991 Moscow (Russian Federation)

[e] V. Y. Kukushkin
Saint Petersburg State Forest Technical University
Institutskii per. 5, 194021 Saint Petersburg (Russian Federation)

Supporting information, including synthetic details, for this article is available on the WWW under http://dx.doi.org/10.1002/cplu.201200257.

Our hypothesis on occurrence of DCA (Scheme 1) was based on the previous reports indicating that pyridinium azomethine ylides in the vast majority of cases (exceptions are known although scarce[22–24]) act as rather reactive 1,3-dipoles toward alkenes with electron-withdrawing groups[25–29] or alkynes[27,28,30–32] (route A) accomplishing, after the oxidative aromatization, the indolizine derivatives.

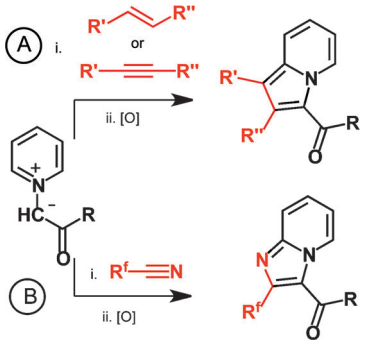

Scheme 1. Cycloaddition of the pyridinium-based azomethine ylides to alkenes, alkynes (A), and nitriles (B) followed by the oxidative aromatization of the ring systems.

Moreover, few examples of DCA of pyridinium azomethine ylides to reactive R^fCN species were also reported (route B in Scheme 1; R = Ar, OAlk; $R_f = CF_3$, C_3F_7, C_7F_{15} in Scheme 2).[33–36]

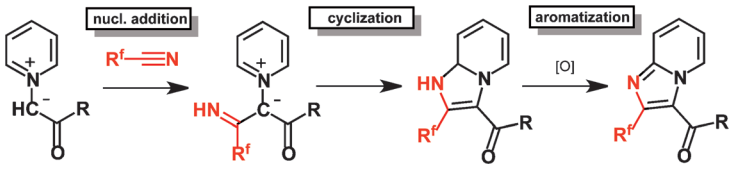

Scheme 2. Presumable mechanism of pyridinium ylide/perfluoronitrile interaction.

The cycloaddition to nitriles is highly unselective and the heterocycles formed were separated in low yields from a broad mixture of CA products and unidentified compounds. In only two studies,[34,36] the products derived from the nucleophilic addition were identified, whereas in other cases[33–36] CA products were isolated. Ten reactions between pyridinium azomethine ylides and the nitrile functionality were reported and they all gave DCA products. However, in four cases, some byproducts derived from the nucleophilic addition were isolated along with DCA adducts; no single example of the selective generation of compounds originating from the nucleophilic addition was described.[36] Based on these observations, the stepwise mechanism that includes the nucleophilic addition followed by the cyclization (but not vice versa) was suggested (Scheme 2).[36]

In contrast to our expectations, we observed that the treatment of the nitrilium borates with azomethine ylides proceeds highly selectively as a nucleophilic addition, rather than DCA, leading to formation of a new carbon–carbon bond and furnishing enamino ketones. The observed reaction—representing the first example of addition of any C-nucleophiles to nitrilium derivatives of boron clusters—is described herein. We also report our theoretical considerations of plausible mechanisms and driving forces of the coupling between free and borylated nitriles with azomethine ylides.

Results and Discussion

Reactivity of 1a–c toward 3a–e

For this study we employed three *closo*-decaborates $[nBu_4N][B_{10}H_9(NCR^1)]$ (**1a**: R^1 = Me; **1b**: R^1 = Et; **1c**: R^1 = Ph) and five azomethine ylides, that is, $p\text{-}R^3C_5H_4N^+CH^-COC_6H_4R^2\text{-}p$ (**2a**: R^3 = H, R^2 = H, X = Br; **2b**: R^3 = H, R^2 = Me, X = I; **2c**: R^3 = H, R^2 = OMe, X = I; **2d**: R^3 = H, R^2 = F, X = I; **2e**: R^3 = Me, R^2 = Me, X = Br). The latter species were generated in situ by the treatment of the corresponding pyridinium salts $[p\text{-}R^3C_5H_4N^+CH_2COC_6H_4R^2\text{-}p](X)$ with Et_3N in accord with the known protocol.[22] The reaction between the nitrile functionality in **1a–c** and azomethine ylides **3a–e** (in all possible combinations) proceeded rapidly in a solution of CH_3NO_2 under mild conditions (RT, 2 min) to afford **4a–o** (ca. quantitative yields based on NMR analysis in $[D_6]$DMSO, 71–87% yield of isolated products for **4a–h,k–n**; Scheme 3. Compound numbering is given in Table 1).

Anionic species **4i**, **4j**, and **4o**, upon removal of the solvent and treatment with methanol, formed the mixed salts $[nBu_4N]_{1-x}[p\text{-}R^3C_5H_4N^+CH_2COC_6H_4R^2\text{-}p]_x[B_{10}H_9\text{-}\{NCR^1{=}C(N^+C_5H_4R^3\text{-}p)COC_6H_4R^2\text{-}p\}]$ with varied ratios between the cations depending on the insignificant differences in the isolation conditions.

The reaction rate is almost independent on the nature of the substituents R^1, R^2, R^3 and it is mostly determined by the rate of dissolution of the borylated nitriles. All isolated compounds **4a–h,k–n** are stable at room temperature both in the solid state and in a solution of $[D_6]$DMSO for at least one month.

Monitoring the reactions with ESI-MS and NMR techniques indicate that under similar reaction conditions (RT, CH_3NO_2) no coupling occurs upon treatment of the electron-deficient nitriles CCl_3CN, MeC(O)CN, and $CHCl_2CN$ with the most reactive azomethine ylide (**2c**) in the presence of Et_3N over a period of three weeks. These data suggest that the C≡N group in the boron clusters is substantially better activated toward the nucleophilic addition as compared to the C≡N group even in electron-deficient nitriles such as R^fCN.

Unlike the reaction of R^fCN, where DCA was observed (see Introduction), pyridinium azomethine ylides undergo nucleophilic addition without cyclization, (Scheme 4, compound **a**: Y = CF_3, C_3F_7; A = NH),[36] to such C-electrophiles as CS_2 in presence of alkylating agent (Scheme 4, compound **b**: Y = S-Alk; A = S),[37] acyl chlorides (Scheme 4, compound **c**: Y = Ar; A = O),[38,39] isocyanates (Scheme 4, compound **d**: Y = NHR; A = O),[39] isothiocyanates (Scheme 4, compound **e**: Y = NHR; A = S),[40] aldehydes (Scheme 4, compound **f**),[41,42] quinolone *N*-oxide (Scheme 4, compound **g**),[43] 2,4,6-trinitrochloroben-

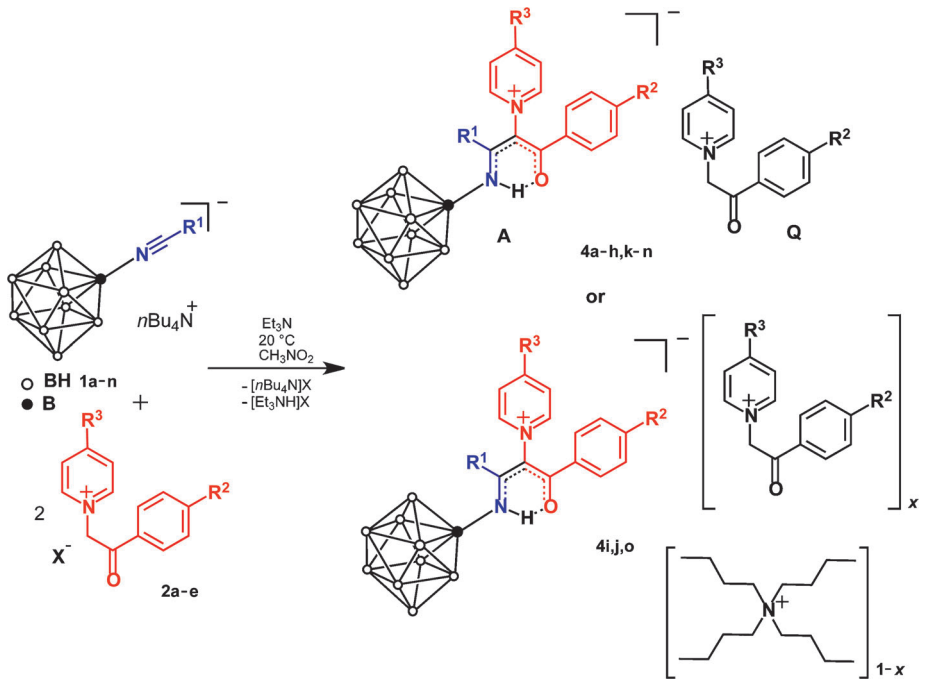

Scheme 3. Synthetic transformations.

Table 1. Compound numbering for the borylated enamino ketones.

Compd	R^1	R^2	R^3	Compd	R^1	R^2	R^3
4a	Me	H	H	**4i**	Et	OMe	H
4b	Me	Me	H	**4j**	Et	Me	Me
4c	Me	F	H	**4k**	Ph	H	H
4d	Me	OMe	H	**4l**	Ph	Me	H
4e	Me	Me	Me	**4m**	Ph	F	H
4f	Et	H	H	**4n**	Ph	OMe	H
4g	Et	Me	H	**4o**	Ph	Me	Me
4h	Et	F	H				

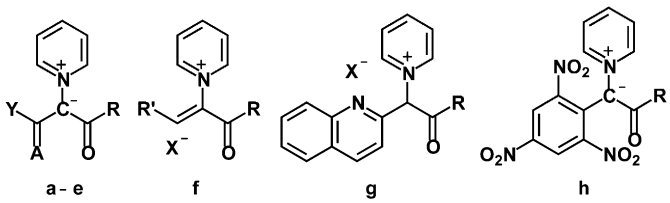

Scheme 4. Products derived from the nucleophilic addition of pyridinium-based azomethine ylides to C-electrophiles.

zene (Scheme 4, compound **h**),[44] and several alkenes (substitution at the C_{sp^2} atom).[45–47] Hence, the reaction reported here represents the first example of the selective nucleophilic addition of pyridinium azomethine ylides to the nitrile group and the first example of new carbon–carbon bond formation in the reaction of nitrilium derivatives of boron clusters with any nucleophiles so far tested.

Characterization of the borylated enamino ketones

All isolated species **4a–h,k–n** were characterized by ICP and high-resolution $ESI^{+/-}$ mass spectrometry, molar conductivity, IR, ^1H, $^{13}C\{^1H\}$, and $^{11}B\{^1H\}$ NMR spectroscopy, and X-ray crystallographic analysis (for **4a** and **4b**). All physicochemical data are in agreement with the proposed formulae. Compounds **4i,j,o** were characterized by high-resolution ESI-MS and ^1H and $^{11}B\{^1H\}$ NMR methods.

The *closo*-decaborate derivatives are hardly combustible to achieve reproducible CHN analyses, therefore all synthesized compounds **4a–h,k–n** were characterized by ICP-mass spectrometry (B%). The obtained compounds give satisfactory ICP-MS-based elemental analysis (see the Supporting Information). In the ESI^- mass spectra of **4a–o**, the most intensive signals correspond to $[A]^-$ and the less intensive ones correspond to $[2A+Q]^-$ (where A^- is the anion and Q^+ is the pyridinium counterion), whereas the ESI^+ mass spectra of **4a–h,k–n** exhibit intensive signals corresponding to $[Q]^+$ and less intensive ones corresponding to $[2Q+A]^+$. For all spectra, the isotopic patterns agree well with the calculated ones. The Λ_M values of **4a–h,k–n** measured solutions of acetonitrile with exact concentration in the range of $2–6\times10^{-4}$ mol L^{-1} are characteristic for ionic species of the $[A]^-[Q]^+$ type in this solvent (measured values: $\Lambda_M = 119–127\ \Omega^{-1}\,cm^2\,mol^{-1}$, typical range:[48] $\Lambda_M = 120–160\ \Omega^{-1}\,cm^2\,mol^{-1}$).

In the IR spectra (see the Supporting Information) of **4a–h,k–n**, the most intensive signals are strong bands corresponding to ν(B–H) vibrations observed in the range of 2451–2515 cm^{-1}, meanwhile strong bands corresponding to ν(C=O) of the cationic part of the molecule were observed in the region of 1681–1703 cm^{-1}. The most characteristic band of each **4a–h,k–n** falls in the range 1335–1340 cm^{-1} and it corresponds to the vibrations of the conjugated system NH-C=C-C=O. No ν(C≡N) bands at approximately 2300 cm^{-1}, specific for the starting nitrilium salts,[4] were observed.

The specific feature of the ^1H NMR spectra (see the Supporting Information) of **4a–o** is the presence of a singlet at $\delta = 11.42–11.13$ ppm from the NH···O group. In the $^{13}C\{^1H\}$ NMR spectra of **4a–h,k–n**, the most characteristic signals are the *C*=O resonance of the anion that fall in the interval of $\delta = 180.6–182.4$ ppm and C=*C*-N peak in the range $\delta = 165.0–171.8$ ppm. The $^{11}B\{^1H\}$ NMR confirmed the *closo*-decaborane structure of **4a–o**. Two singlets from the apical boron atoms B^{10} and B^1 were observed in the range $\delta = 0.5–1.0$ ppm and

from $\delta = -0.6$ to -1.0 ppm, respectively, the weak broad singlet of the substituted boron atom B^2 was found between $\delta = -12.6$ and -13.7 ppm, and the other equatorial atoms emerged as a multiple signal in the intervals between $\delta = -23.7$ and -24.2 ppm (B^3, B^5, B^6, B^9), and $\delta = -26.0$ and -27.5 ppm (B^4, B^7, B^8). All signals of the unsubstituted boron atoms split into doublets without the broadband ^{1}H decoupling, whereas the substituted B^2 atom still gives the singlet signal.

The single-crystal X-ray analysis of **4a** and **4b** (Figure 1 and Figure S1 in the Supporting Information) disclose the presence of two independent ionic parts. All bond lengths and angles of the cationic part are the same, within 3σ, as those described in the literature.[49] The anionic parts of **4a** and **4b** consist of the *closo*-decaborate cluster bound to the organic fragment through the N1 atom. In the cluster part, the B–B bond distances and angles are typical for 2-substituted nonahydro-*closo*-decaboron clusters.[4,50] The bond lengths N1–B2 are equal, within 3σ, to those in the starting borylated nitrile.[50] The geometry of the anionic part of the molecule is determined by hydrogen bonding, N1–H···O1, giving a slightly distorted planar six-membered system H-N1-C1-C3-C9-O1. The bond lengths N1–C1, C1–C3, C3–C9, and C9–O1 (see Table 2) of this system are intermediate between the reported values for the corresponding standard single and double bonds.[51] The bond lengths and angles are very close to similar systems observed previously.[52–54] Owing to the hydrogen bonding N1–H···O1 and the planarity of the H-N1-C1-C3-C9-O1 system, the aromatic rings are sterically hindered. The torsion angle O1-C9-C10-C11 is 58.8° for **4a** and 51.4° for **4b** and, consequently, the carbonyl group is extensively turned away from conjugation with the phenyl ring. This observation obviously explains the unconventional chemical shifts of CO-$C_6H_4R^2$-*p* in the ^{1}H NMR spectra of the anionic part of **4a–o**. The pyridinium ring is turned at 69.9° for **4a** and 69.2° for **4b** with respect to the plane C1-C3-C9 and does not conjugate with the system H-N1-C1-C3-C9-O1. All other bonds and angles have expected values.

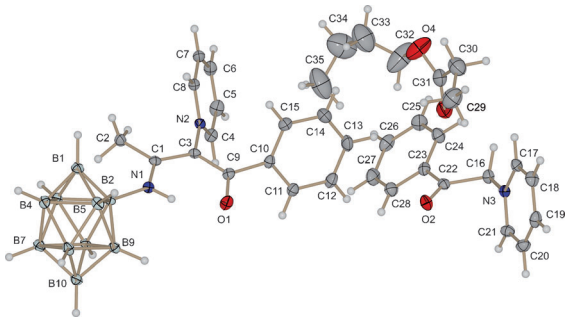

Figure 1. ORTEP view of **4a** with the atom numbering. The thermal ellipsoids are drawn at the 30% probability level.

Table 2. Selected bond lengths [Å] and dihedral angles [°] for **4a** and **4b**.

Bond lengths	Compounds **4a**	Compounds **4b**	Angles	Compounds **4a**	Compounds **4b**
N1–B2	1.522(2)	1.523(4)	C1-N1-B2	130.60(16)	131.5(2)
N1–C1	1.311(2)	1.315(3)	N1-C1-C3	119.96(16)	120.9(2)
C1–C3	1.420(2)	1.412(4)	C1-C3-C9	124.91(16)	125.6(2)
C3–C9	1.408(3)	1.406(4)	C3-C9-O1	122.36(16)	121.0(3)
O1–C9	1.256(2)	1.262(3)	N1-C1-C2	118.63(16)	117.4(3)
C1–C2	1.492(3)	1.494(4)	C3-C1-C2	121.37(16)	121.6(2)
N2–C3	1.452(2)	1.463(3)	C1-C3-N2	117.33(15)	117.1(2)
C9–C10	1.502(2)	1.492(4)	C9-C3-N2	117.73(15)	117.2(2)
			C3-C9-C10	120.72(16)	121.3(2)
			O1-C9-C10	116.92(16)	117.7(3)

Theoretical considerations and reaction mechanism

With an aim to interpret and explain the experimental observations, quantum chemical calculations of the plausible reactions mechanisms of both cycloaddition and nucleophilic addition of free and borylated nitriles [N≡CMe and $[B_{10}H_9(N{\equiv}CMe)]^-$ (**I**)] with the azomethine ylide $C_5H_5N^+CH^-C(O)Me$ (**II**) have been performed at the DFT level. Two main questions were raised, that is, 1) why are the borylated nitriles much more active toward the azomethine ylides than free N≡CR and 2) why does the reaction between borylated nitriles and azomethine ylides affords the nucleophilic addition product instead of a cycloadduct?

Cycloaddition of II to nitriles

Reaction mechanism

For this reaction, there are two regioisomeric pathways leading to 5-acyl (**III1**, **IV1**) and 2-acyl (**III2**, **IV2**) 2,5-dihydro-1*H*-imidazoles (Scheme 5). Within each regioisomeric pathway, two stereoisomers may be formed [**III1a(b)**, **III2a(b)**, **IV1a(b)**, and **IV2a(b)**. Finally, the formation of two conformers with different position of the C(O)Me substituent relative to the heterocycle is possible for each stereoisomer except **III2a** for which only one conformer **III2a2** was found.

For CA of **II** to N≡CMe or **I**, transition states of a concerted mechanism were located for each reaction pathway except for that leading to **IV1a2** (Figure 2 and **Figure S2**). At the same time, isomer **IV1a2** can be easily formed from **IV1a1** upon rotation around the carbon–carbon bond (Scheme 5). Besides, two stepwise pathways were found for CA of **II** to **I** involving the generation of acyclic intermediates **INTIV1a1** or **INTIV2a2** and leading to the CA products **IV1a1** and **IV2a2**, respectively (Scheme 6). The second steps (ring closure) are rate determining. No stepwise route exists for the reaction of **II** with N≡CMe.

Kinetic factors

The calculated activation energy (in terms of $\Delta G_s^{\neq}$) is lowest for the pathway that affords isomers **III1b1** and **IV1b1** (Table 3). For the reaction between N≡CMe and **II**, the corre-

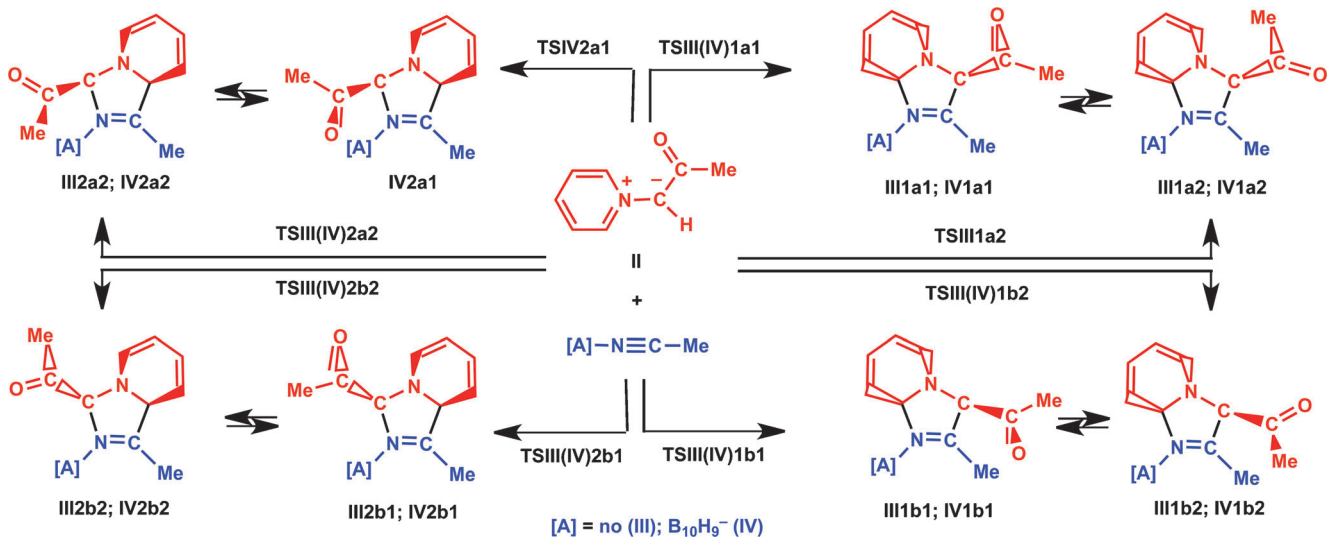

Scheme 5. 1,3-Dipolar cycloaddition of azomethine ylide **II** to N≡CMe and $[B_{10}H_9(N{\equiv}CMe)]^-$ (**I**; transition states of the concerted mechanisms are indicated).

sponding $\Delta G_s^{\neq}$ value is 33.9 kcal mol^{-1}. This value is higher than $\Delta G_s^{\neq}$ for the reactions of N≡CMe with the simple acyclic azomethine ylide $CH_2{=}N^+(Me)CH_2^-$ (19.0 kcal mol^{-1}) and with the nitrone $CH_2{=}N^+(Me)O^-$ (31.5 kcal mol^{-1}) in a solution of CH_2Cl_2.[55–58] Taking into account that N≡CMe does not react with acyclic nitrones,[59,60] its reaction with **II** is also not expected, in accordance with the experimental observations (see above).

The lowest activation barrier to CA of **II** to **I** is 21.1 kcal mol^{-1}. This is 12.8 kcal mol^{-1} lower than the $\Delta G_s^{\neq}$ value of the boron-free reaction and corresponds to an enhancement of the reaction rate by a factor of 2.5×10^9! Thus, the binding of the N≡C group to the B atom results in a dramatic activation of nitriles toward CA with azomethine ylides, and the reaction **II**+**I** is quite favorable kinetically. The second regioisomeric pathway (i.e. that yielding isomers **III2** and **IV2**) is clearly less favorable.

Synchronicity

Another important characteristic of the concerted mechanism is the degree of its synchronicity. The most reliable criterion of the synchronicity is based on the estimate of parameter S_y, which may vary from 0 (stepwise mechanism) to 1 (completely synchronous CA; see computational details in the Experimental Section). The S_y value of CA **II**+N≡CMe is 0.70 (the **III1b1** pathway) indicating that the mechanism is asynchronous by 30%. The coordination of N≡CMe to $[B_{10}H_9]^-$ leads to a significant increase of the asynchronicity to $S_y=0.54$ with the formation of the carbon–carbon bond preceding the carbon–nitrogen bond making. Such an increase of the asynchronicity is accounted for by significant steric repulsions between the pyridine ring and the boron cluster in **TSIV1b1** (Figure 2).

Thermodynamic factors

The calculations demonstrate that isomers **III1b2** and **IV1b2** are the most thermodynamically stable among the others. They can be easily formed from the most kinetically accessible isomers **III1b1** and **IV1b1** upon rotation around the carbon–carbon bond. At the same time, the energies of all other isomers are higher only by 0.7–4.3 kcal mol^{-1} (Table 3). The Gibbs free energies of the formation of all isomers **III** and **IV** in a CH_3NO_2 solution (ΔG_s) are significantly positive (9.6–15.2 kcal mol^{-1}). Thus, CA of **II** to both N≡CMe and **I** is not favorable thermodynamically, and generation of CA products upon the reaction of **II** with **I** is not expected despite the comparatively low activation barrier of this process, in agreement with the experimental data (see above).

Nucleophilic addition of II to nitriles

Concerted mechanism

For the nucleophilic addition reactions (NAs) to nitriles, three general types of mechanism may be considered, that is, concerted, associative, and dissociative. The first one (Scheme 7) includes the formation of a new carbon–carbon bond and the hydrogen transfer from the azomethine carbon atom to the nitrile nitrogen in a single step via one cyclic transition state. This transition state may be either four-membered (type a) or six-membered (type b). In the latter case, a solvent molecule participates in the formation of TS and plays the role of the hydrogen-transfer promoter. Taking into account that the solvent used in the experimental part (nitromethane) was not dried and, hence, contains some water, namely H_2O was considered as the hydrogen-transfer promoter in TSs of type b (however, the bulky solvent effect was calculated at the CPCM level for CH_3NO_2 as solvent, see computational details in the Experimental Section).

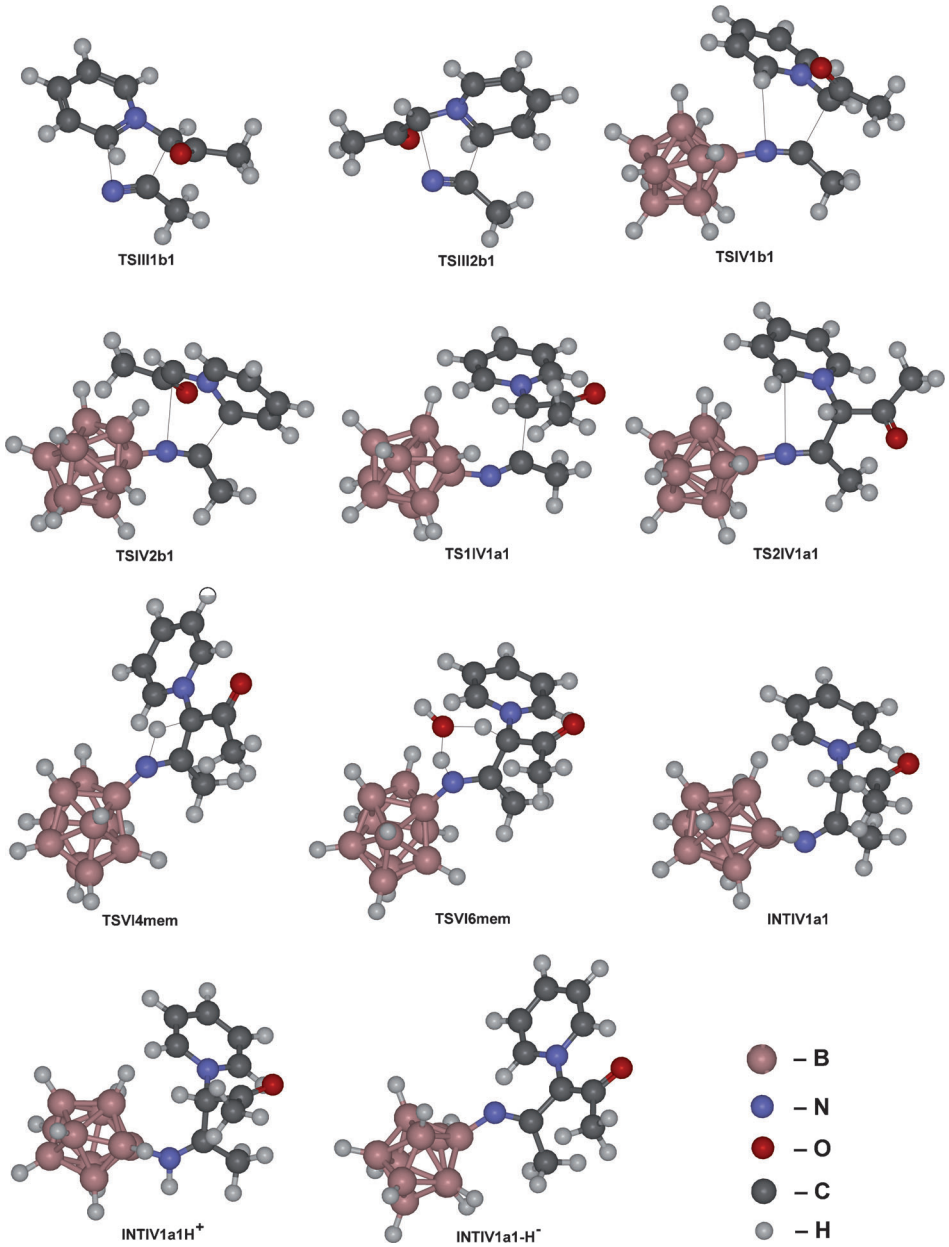

Figure 2. Equilibrium geometries of selected transition states and intermediates.

Transition states of both types a and b (**TSV4mem**, **TSV6mem**, **TSVI4mem**, and **TSVI6mem**) were found for concerted NAs (Figure 2). The activation barriers of the reactions via the four-membered transition states are significantly higher than those via the six-membered TSs (Table 3). This finding is not surprising considering the fact that six-membered structures are usually more stable than four-membered ones. The barrier of the nucleophilic addition **II**+N≡CMe via **TSV6mem** is 45.9 kcal mol^{-1}, which is too high for an effective realization of this route. The activation energy of the reaction **II**+**I** via **TSVI6mem** is 24.3 kcal mol^{-1}, which is quite acceptable for occurrence of the reaction. However, this value is higher than the barrier found for the CA route between **II** and **I** (21.1 kcal mol^{-1}). Hence, NA via a concerted mechanism should be less favorable than CA, thus contradicting the experimental findings.

Associative mechanism

The associative mechanism of NA to nitriles (Scheme 8) involves the addition of the nucleophile to the nitrile carbon atom and subsequent two-step proton transfer via either route A or route B. As was mentioned above, no acyclic intermediate was found for the reaction of **II** with N≡CMe. However, in the case of NA of **II** to **I**, two intermediates **INTIV1a1** and **INTIV2a2** were located. In fact, these species represent the acyclic intermediates of the stepwise cycloaddition discussed above (Scheme 6). The activation energy for the formation of **INTIV1a1** (19.6 kcal mol^{-1}) is significantly lower than that of **INTIV2a2** (Table 3).

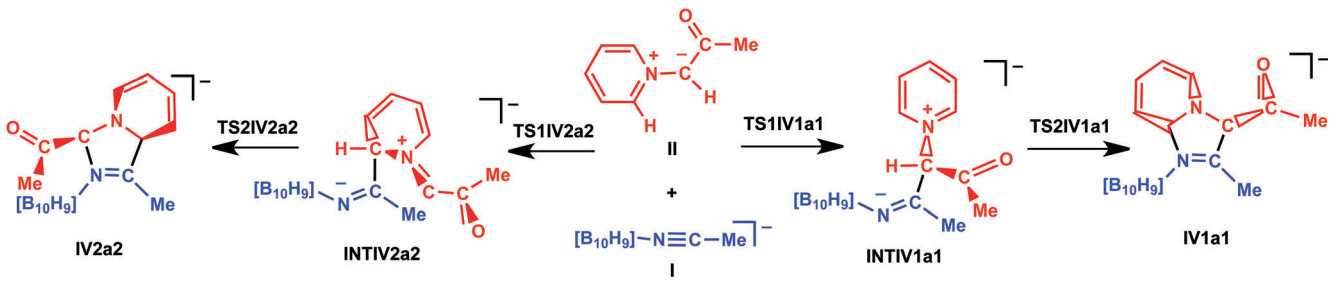

Scheme 6. Stepwise mechanisms of cycloaddition of **II** to **I**.

Table 3. Calculated Gibbs free energies of activation and reaction in a solution of CH_3NO_2.

Reaction	$\Delta G_s^{\neq}$ [kcal mol^{-1}]	ΔG_s [kcal mol^{-1}]
N≡CMe + **II** → **III1a1** via **TSIII1a1**	36.1	15.2
N≡CMe + **II** → **III1a2** via **TSIII1a2**	40.6	14.3
N≡CMe + **II** → **III1b1** via **TSIII1b1**	33.9	14.3
N≡CMe + **II** → **III1b2** via **TSIII1b2**	36.3	12.8
N≡CMe + **II** → **III2a2** via **TSIII2a2**	45.8	15.1
N≡CMe + **II** → **III2b1** via **TSIII2b1**	41.3	13.8
N≡CMe + **II** → **III2b2** via **TSIII2b2**	46.7	14.3
I + **II** → **IV1a1** via **TSIV1a1**	21.5	13.8
I + **II** → **IV1a2**	–	12.4
I + **II** → **IV1b1** via **TSIV1b1**	21.1	13.4
I + **II** → **IV1b2** via **TSIV1b2**	24.9	9.6
I + **II** → **IV2a1** via **TSIV2a1**	39.0	13.7
I + **II** → **IV2a2** via **TSIV2a2**	47.0	11.4
I + **II** → **IV2b1** via **TSIV2b1**	38.3	10.5
I + **II** → **IV2b2** via **TSIV2b2**	52.1	10.2
I + **II** → **INTIV1a1** via **TS1IV1a1**	19.6	11.6
INTIV1a1 → **IV1a1** via **TS2IV1a1**	16.1	2.3
I + **II** → **INTIV2a2** via **TS1IV2a2**	45.5	46.6
INTIV2a2 → **IV2a2** via **TS2IV2a2**	3.1	−35.3
N≡CMe + **II** → **V** via **TSV4mem**	68.0	14.4
N≡CMe + **II** → **V** via **TSV6mem**	45.9	14.4
I + **II** → **V** via **TSVI4mem**	44.3	−3.6
I + **II** → **V** via **TSVI6mem**	24.3	−3.6
INTIV1a1 + H_2O → **INTIV1a1-H**$^-$ + H_3O^+	–	54.9
INTIV1a1 + Me_3N → **INTIV1a1-H**$^-$ + Me_3NH^+	–	29.3
INTIV1a1 + **II** → **INTIV1a1-H**$^-$ + **II**$^+$	–	15.9
INTIV1a1 + Me_3NH^+ → **INTIV1a1H**$^+$ + Me_3N	–	−14.0
INTIV1a1H$^+$ + Me_3N → **V** + Me_3NH^+	–	−1.2

In accord with route A (Scheme 8), intermediate **INTIV1a1** should undergo deprotonation. The reactions **INTIV1a1** + B → **INTIV1a1-H**$^-$ + BH^+ are still endoergonic by 54.9, 29.3, and 15.9 kcal mol^{-1}, for B = H_2O, Me_3N, and **II**, respectively. However, the azomethine C–H bond in **INTIV1a1** is significantly more acidic than that in **II**. Within route B (Scheme 8), the protonation of **INTIV1a1** should occur first, and the calculations demonstrate that the process **INTIV1a1** + Me_3NH^+ → **INTIV1a1H**$^+$ + Me_3N is exoergonic by 14.0 kcal mol^{-1} (Me_3NH^+ is formed upon the in situ generation of the azomethine ylide; see the Experimetal Section). Thus, the protonation of **INTIV1a1** is much more favorable compared to its deprotonation.

The proton elimination from the former ylide fragment in **INTIV1a1H**$^+$ leads to the final experimentally isolated NA product **V** and this step is also exoergonic by 1.2 kcal mol^{-1}. Note that the ring closure in **INTIV1a1** to give **IV1a1** (Scheme 6) requires overcoming an activation barrier of 16.1 kcal mol^{-1}.

The overall activation barrier of NA **I** + **II** → **V** via the associative mechanism (route A) is 19.6 kcal mol^{-1}, the formation of **INTIV1a1** is the rate limiting step (Figure 3). This value is lower than the activation energies of both concerted NA (24.3 kcal mol^{-1}) and CA (21.1 kcal mol^{-1}), thus, correlating with the experimental formation of the NA product instead of the CA one. However, the main driving force determining the direction of the reaction of **II** with **I** has a thermodynamic rather than a kinetic nature. Indeed, the ΔG_s value of NA **II** + **I** → **V** is negative (−3.6 kcal mol^{-1}), whereas the reaction energy of CA **II** + **I** → **IV1b2** is clearly positive (9.6 kcal mol^{-1}).

Besides, the dissociative mechanism of NA of **II** to nitriles was also considered but found to be highly unfavorable (see the Supporting Information for details).

Factors controlling the reactivity of the borylated and the boron-free nitriles toward II

Steric factor

The presence of a bulky substituent such as $[B_{10}H_9]^-$ at the nitrile nitrogen atom provides a strong steric repulsion between the boron cluster and the approaching ylide upon the reaction of **I** with **II**. This steric effect dramatically increases the asyn-

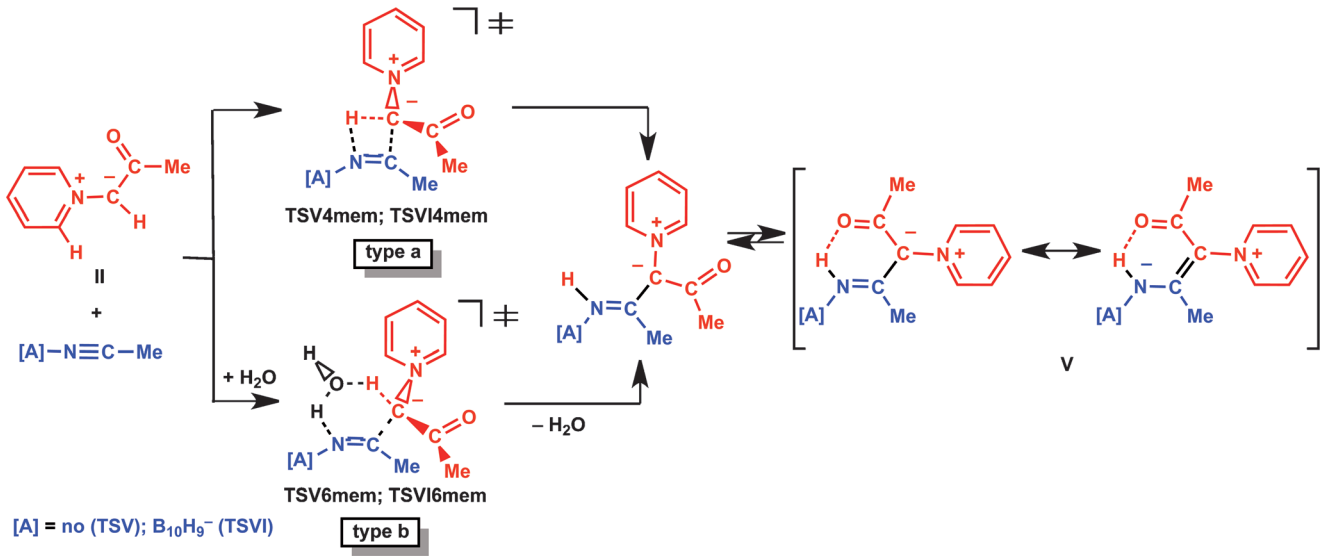

Scheme 7. Concerted mechanism of nucleophilic addition of **II** to nitriles.

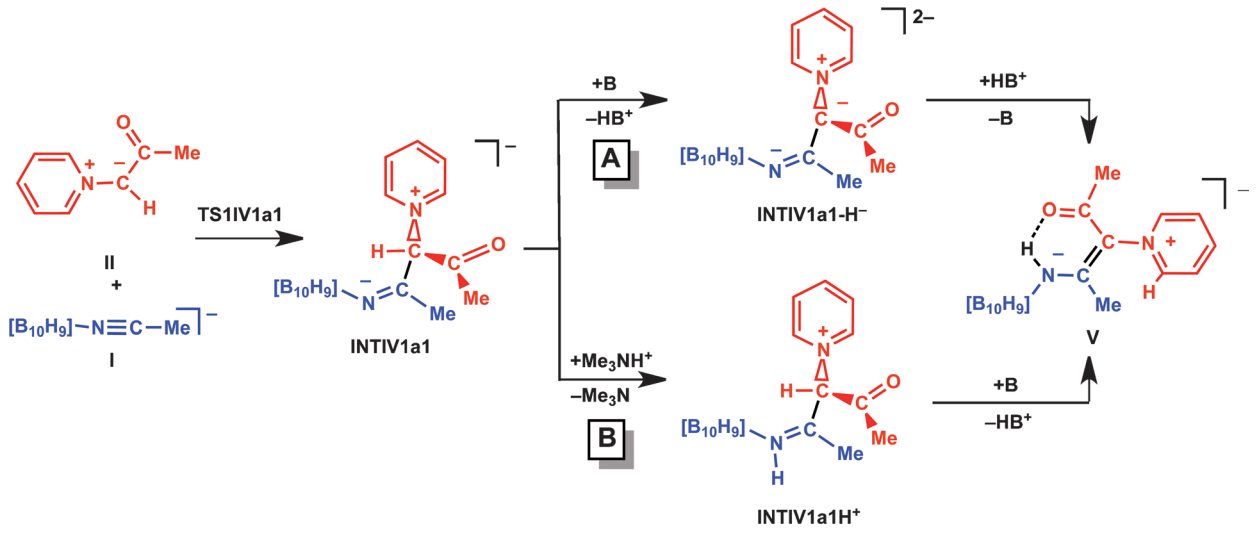

Scheme 8. Associative mechanism of nucleophilic addition of **II** to **I**.

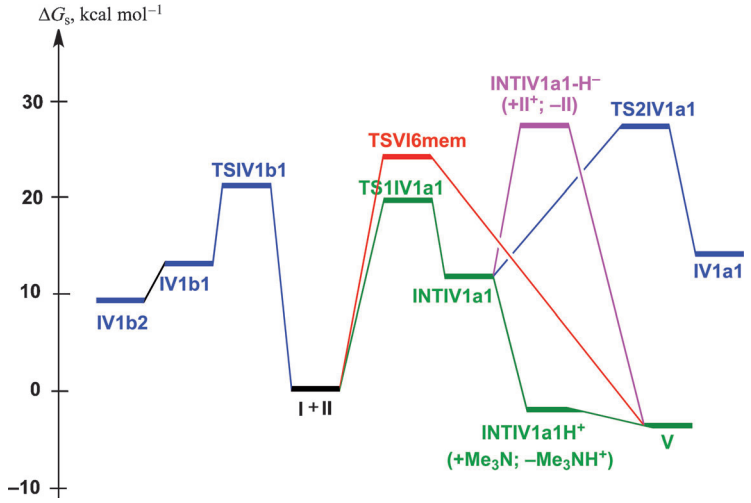

Figure 3. Energy profiles of some reaction pathways: stepwise nucleophilic additions in green (the most favorable route) and magenta (less favorable route), concerted nucleophilic addition in red, and cycloadditions in blue].

chronicity of the process, thus hampering the carbon–nitrogen bond formation and facilitating creation of the carbon–carbon bond. As a result, the generation of the acyclic intermediate **INTIV1a1** further converting to NA product **V** becomes possible and favorable for the borylated nitrile; although no species of such type can be formed in the case of acetonitrile. Moreover, the steric repulsion upon the formation of the carbon–nitrogen bond makes CA products **IV** thermodynamically unstable compared to NA product **V**.

Molecular orbital composition and energies

In terms of the frontier molecular orbital (FMO) theory, the NA reactions are controlled by the interaction of the HOMO of the nucleophile and of the LUMO of the substrate. For the CA reactions, three main groups may be distinguished in accord with the classification by Sustmann,[61,62] that is, group I (normal electron demand processes with the predominant $HOMO_{dipole}$–$LUMO_{dipolarophile}$ interaction), group III (inverse electron demand reactions with the prevailing $HOMO_{dipolarophile}$–$LUMO_{dipole}$ interaction), and group II ("neutral" processes with both HOMO–LUMO interactions efficiently operating).

The analysis of the FMO energies and composition indicates that CA of **II** to N≡CMe is clearly a normal electron demand process (Figure 4). Thus, for a given dipole, the reactivity of nitrile should depend on its LUMO energy.

Several highest occupied MOs of **I** are localized on the $B_{10}H_9$ fragment while the first occupied MO centered on the C≡N bond [π(C≡N)] is HOMO-16. The first unoccupied MO corresponding to π*(C≡N) is the LUMO (Figure 5). The binding of N≡CMe with the B atom at $[B_{10}H_9]^-$ results in an increase of the energies of both π(C≡N) and π*(C≡N) because of acquired overall negative charge of **I**. As a result, both $HOMO_{ylide}$–$LUMO_I$ and $HOMO\text{-}16_I$–$LUMO_{ylide}$ gaps become similar (6.85 and 6.58 eV, respectively) and CA of **II** to **I** belongs to group II. It is interesting that the smallest HOMO(C≡N)–LUMO gap increases ongoing from N≡CMe (5.84 eV) to **I** (6.58 eV; Figure 4), and a lower reactivity of **I** is expected compared to N≡CMe. This finding contradicts the experimental data and the computational results discussed above and, thus, demonstrates that the FMO theory fails to predict correctly the reactivity of the systems under study.

Effective atomic charges

Another factor which controls the reactivity of the nitriles toward **II** is the effective atomic charge on the reacting atoms. Taking into account that CA of **II** to **I** is asynchronous with the prior formation of the carbon–carbon bond, namely the charge on the nitrile C atom is crucial for both CA and NA pathways. The calculations indicate that the NBO atomic

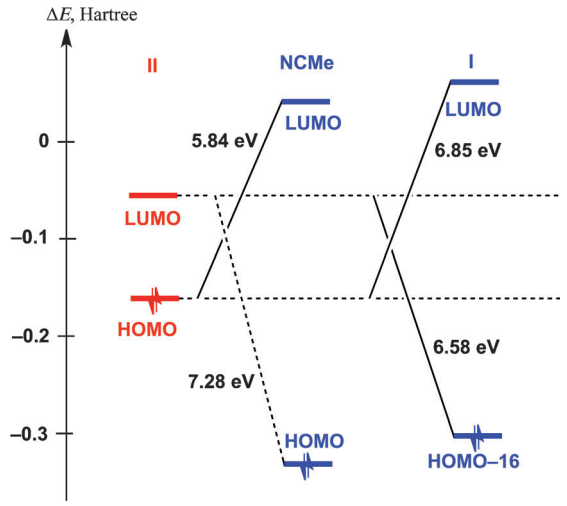

Figure 4. Relative energies of the interacting HOMOs and LUMOs of reactants (the HOMO–LUMO gaps are indicated in eV).

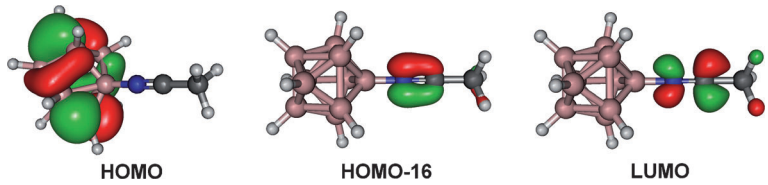

Figure 5. Plots of selected frontier molecular orbitals.

charge on the nitrile C atom dramatically increases upon binding of N≡CMe with $[B_{10}H_9]^-$ (from 0.28 e to 0.45 e). Such an enhancement should facilitate the attack of a nucleophile (or of a nucleophilic center of 1,3-dipole) at the nitrile C atom. Thus, the great activation of the nitriles upon borylation may be explained in terms of electrostatic arguments. It is also interesting that the charge on the nitrile N atom becomes less negative (from −0.33 e in N≡CMe to −0.24 e in **I**). Therefore, the borylation results in a release of the electron density from the entire C≡N group of nitriles.

Conclusion

We observed the novel reaction between the *closo*-decaborate clusters $[n\mathrm{Bu}_4\mathrm{N}][B_{10}H_9(\mathrm{NCR}^1)]$ and the azomethine ylides, which selectively affords products of the nucleophilic addition, that is, the borylated enamino ketones $[B_{10}H_9\{\mathrm{NCR}^1{=}\mathrm{C}(\mathrm{N}^+\mathrm{C}_5\mathrm{H}_4\mathrm{R}^3\text{-}p)\mathrm{COC}_6\mathrm{H}_4\mathrm{R}^2\text{-}p\}]^-$, and no species derived from DCA was detected. This coupling represents the first example of new carbon–carbon bond making in the reaction of nitrilium derivatives of boron clusters with any nucleophile so far tested. The formation of new carbon–carbon bonds is of central importance in organic chemistry as skeleton-forming processes. In main group element chemistry, the studied reaction provides an easy access to modification of boron clusters under mild conditions and this is useful for, for example medicinal chemistry and for syntheses of libraries of potential agents for the boron neutron capture therapy.[1,2,63] This reaction also represents the first example of the nucleophilic addition of phenacyl pyridinium-based azomethine ylides to the nitrile functionality.

To explain the selectivity of the reaction (nucleophilic addition vs. cycloaddition), we studied the reactivity of the free and the borylated nitriles, N≡CMe and $[B_{10}H_9(\mathrm{N{\equiv}CMe})]^-$ (**I**), toward the azomethine ylide $C_5H_5N^+CH^-C(O)Me$ (**II**) by theoretical (DFT) methods. The calculations indicate that DCA of **II** either to N≡CMe or to **I** is clearly thermodynamically unfavorable ($\Delta G_s = +12.8$ and $+9.6$ kcal mol^{-1}, respectively). However, different activation barriers (33.9 vs. 21.1 kcal mol^{-1}, correspondingly) indicate the significant kinetic activation of N≡CMe upon its binding to $[B_{10}H_9]^-$. Such activation can be accounted for in terms of electrostatic arguments as a result of an increase of the positive atomic charge on the C nitrile atom ongoing from N≡CMe to **I**, while the FMO theory fails to explain this effect.

The nucleophilic addition of **II** to **I** is exoergonic by −3.6 kcal mol^{-1}, with slightly lower activation barrier compared to the CA pathway (19.6 kcal mol^{-1}). Thus, the experimentally observed formation of the nucleophilic addition product instead of CA adduct can be rationalized by the thermodynamic factors rather than by the kinetic arguments. The lower thermodynamic stability of CA adduct compared to NA product is explained by the steric repulsion between the bulky $[B_{10}H_9]^-$ cluster and the ylide molecule. The mechanism of NA of **II** to **I** is associative and includes the generation of acyclic intermediate **INTIV1a1**, the protonation of the nitrile N atom leading to **INTIV1a1H$^+$**, and deprotonation of the C atom to finally afford **V**.

The ability to isolate enamino ketones from the reactions between the *closo*-decaborate clusters and the azomethine ylides gives us the opportunity to prepare new classes of boron-containing bidentate ligands for use in the areas of coordination and organometallic chemistry. The complexation of these chelates with metal centers (for recent studies see Refs. [64–68]) generating complexes functionalized with the *closo*-decaborate moiety should open up yet another method for facile derivatization of the boron clusters and research in this direction is currently underway by our group.

Experimental Section

Instrumentation and Materials

The reagents RC_6H_4COMe (R = H, F: Acros Organics; Me, OMe: Alfa Aesar), pyridine, 4-picoline, and the employed solvents were obtained from commercial sources and used as received. *closo*-Decaborate clusters **1a**,[69] **1b**, **1c**,[11] and **1d**[6] were prepared in accord with the published methods. Pyridinium salts **2b**, **2b**, and **2c** were synthesized by reaction of the substituted acetophenone with pyridine in the presence of iodine by using known protocols,[70] **2a** and **2d** were prepared by reaction of the corresponding α-bro-

moacetophenone with pyridine or 4-picoline.[42] $RC_6H_4COCH_2Br$ (R = H, Me) were obtained accordingly to known protocols.[71]

Elemental analysis for boron was performed by the FSUE IREA 291 Center (Moscow) on a iCAP 6300 Duo ICP spectrometer using In as 292 an internal standard. Infrared spectra were recorded on a Shimadzu FTIR 8400S instrument in KBr pellets. ^{1}H, ^{13}C{^{1}H}, and ^{11}B{^{1}H} NMR spectra were measured on a Bruker-DPX 300 spectrometer at ambient temperature; $BF_3{\cdot}Et_2O$ was used as the external standard for ^{11}B{^{1}H} NMR analysis. Electrospray ionization mass spectra were obtained on a Bruker micrOTOF spectrometer equipped with electrospray ionization (ESI) source and MeOH or MeCN were used as the solvents. The instrument was operated both at positive and negative ion modes using a *m/z* range of 50–3000. In the isotopic pattern, the most abundant peak is reported. Molar conductivities of 10^{-3}–10^{-4} M solutions in acetonitrile were measured on a Mettler Toledo conductometer FE30 using Inlab 710 sensor. Melting points were determined in a capillary on a Büchi Melting Point 530 Apparatus.

X-ray diffraction studies

The crystals of complexes **4a** and **4b** were immersed in cryo-oil, mounted in a Nylon loop, and measured at a temperature of 100 K or 120 K. The X-ray diffraction data were collected on a Bruker Smart Apex II or Bruker Kappa Apex II Duo diffractometer using $Mo_{K\alpha}$ radiation (λ = 0.71073 Å). The APEX2[72] software package was used for cell refinements and data reductions. The structures were solved by direct methods using the SHELXS-97[73] program with the Olex2[74] graphical user interface. A semiempirical absorption correction (SADABS)[75] was applied to all data. Structural refinements were carried out using SHELXL-97.[73] The crystal of **4b** was diffracting only weakly. The butyl propionate of crystallization was heavily disordered and therefore omitted from the final structure model. The contribution of the disordered solvent to the calculated structure factors was taken into account by using the solvent mask routine of Olex2.[74] The missing solvent was also taken into account in the unit cell content. In structure **4a** the NH hydrogen atom was located from the difference Fourier and refined isotropically. All other hydrogen atoms were positioned geometrically and constrained to ride on their parent atoms, with C–H = 0.95–0.99 Å, N–H = 0.88 Å, B–H = 1.12 Å, and U_{iso} = 1.2–1.5 U_{eq} (parent atom). The crystallographic details are summarized in Table 4. CCDC 902348 (**4a**) and 902349 (**4b**) contain the supplementary crystallographic data for this paper. These data can be obtained free of charge from The Cambridge Crystallographic Data Centre via www.ccdc.cam.ac.uk/data_request/cif.

Computational details

The full geometry optimization of all structures and transition states has been carried out at the DFT/HF hybrid level of theory using Becke's three-parameter hybrid exchange functional in combination with the gradient-corrected correlation functional of Lee, Yang and Parr (B3LYP)[76,77] with the help of the Gaussian-03[78] program package. No symmetry operations have been applied. The geometry optimization was carried out using the 6–31G(d) basis set followed by the single-point calculations with the 6–311+G(d,p) basis set. As was shown previously,[55–58] this approach is sufficiently accurate for the description of CAs to the C≡N bond providing results close to those obtained by such methods as MP2, MP4, CCSD(T), CBS-Q, and G3B3.

Table 4. Crystal Data.

	4a	4b
formula	$C_{35}H_{49}B_{10}N_3O_4$	$C_{37}H_{53}B_{10}N_3O_4$
Mr	683.87	711.92
T (K)	100(2)	120(2)
λ(Å)	0.71073	0.71073
crystal system	Triclinic	Triclinic
space group	$P\bar{1}$	$P\bar{1}$
a [Å]	8.3048(10)	8.3414(15)
b [Å]	14.3736(17)	14.338(3)
c [Å]	17.191(2)	16.561(3)
α [deg]	109.546(6)	93.244(6)
β [deg]	95.222(7)	96.105(5)
γ [deg]	100.532(7)	100.330(6)
V [Å^3]	1875.4(4)	1931.8(6)
Z	2	2
ρ_{calc} [Mg cm^{-3}]	1.211	1.224
$\mu(Mo_{K\alpha})$ [mm^{-1}]	0.073	0.074
No. reflns.	47852	24572
unique reflns.	9344	6779
GOOF (F^2)	1.024	0.901
R_{int}	0.0534	0.0824
R_1[a] ($I \geq 2\sigma$)	0.0588	0.0667
wR_2[b] ($I \geq 2\sigma$)	0.0994	0.1457

[a] $R_1 = \Sigma||F_o|-|F_c||/\Sigma|F_o|$. [b] $wR_2 = [\Sigma[w(F_o^2-F_c^2)^2]/\Sigma[w(F_o^2)^2]]^{1/2}$.

The Hessian matrix was calculated analytically for the optimized structures to prove the location of correct minima (no imaginary frequencies) or saddle points (only one imaginary frequency), and to estimate the thermodynamic parameters, the latter being calculated at 25 °C. The nature of all transition states was investigated by the analysis of vectors associated with the imaginary frequency and by the calculations of the intrinsic reaction coordinates (IRC) using the Gonzalez-Schlegel method.[79–81] Sometimes, the IRC calculations failed due to low imaginary frequency of a transition state. In these cases, the analysis of the TS nature was performed in accord with the following procedure. First, the atoms of TS were shifted from the equilibrium positions along the vectors corresponding to the imaginary frequency, in both directions. Then, geometry optimization with small size of an optimization step was carried out.

Total energies corrected for solvent effects (E_s) were estimated at the single-point calculations on the basis of gas-phase geometries at the CPCM-B3LYP/6–311+G(d,p)//gas-B3LYP/6–31G(d) level of theory using the polarizable continuum model in the CPCM version[82,83] with CH_3NO_2 as solvent. The UAKS model was applied for the molecular cavity. The entropic term in solution (S_s) was calculated according to the procedure described by Wertz[84] and Cooper and Ziegler[85] using [Eqs. (1)–(4)]

$$\Delta S_1 = R\ln V^s_{m,liq}/V_{m,gas} \quad (1)$$

$$\Delta S_2 = R\ln V^o_m/V^s_{m,liq} \quad (2)$$

$$\alpha = \frac{S^{o,s}_{liq} - \left(S^{o,s}_{gas} + R\ln V^s_{m,liq}/V_{m,gas}\right)}{\left(S^{o,s}_{gas} + R\ln V^s_{m,liq}/V_{m,gas}\right)} \quad (3)$$

$$S_s = S_g + \Delta S_{sol} = S_g + [\Delta S_1 + \alpha(S_g + \Delta S_1) + \Delta S_2] = S_g + [(-12.16\ \text{cal mol}^{-1}\ \text{K})\text{-}0.233(S_g - 12.16\ \text{cal mol}^{-1}\ \text{K}) + 5.81\ \text{cal mol}^{-1}\ \text{K}] \quad (4)$$

where S_g = gas-phase entropy of solute, ΔS_{sol} = solvation entropy, $S^{\circ,s}_{liq}$, $S^{\circ,s}_{gas}$, and $V^s_{m,liq}$ = standard entropies and molar volume of the solvent in liquid or gas phases (171.8 and 275.0 J mol^{-1} K and 53.65 mL mol^{-1}, respectively, for CH_3NO_2), $V_{m,gas}$ = molar volume of the ideal gas at 25 °C (24450 mL mol^{-1}), V°_m = molar volume of the solution corresponding to the standard conditions (1000 mL mol^{-1}). The enthalpies and Gibbs free energies in solution (H_s and G_s) were estimated using the [Eqs. (5) and (6)]

$$H_s = E_s(\text{6-311} + \text{G(d,p)}) - E_g(\text{6-311} + \text{G(d,p)}) + H_g(\text{6-31G(d)}) \quad (5)$$

$$G_s = H_s - \text{TS}_s \quad (6)$$

where E_s, E_g and H_g are the total energies in solution and in gas phase and gas-phase enthalpy calculated at the corresponding level.

The atomic charges were computed by using the natural bond orbital (NBO) partitioning scheme.[86] The synchronicity of CAs (S_y) was calculated using the formula:[87–90]

$$S_y = 1 - (2n-2)^{-1} \cdot \sum_{i=1}^{n} \frac{\delta B_i - \delta B_{av}}{\delta B_{av}} \quad (7)$$

where n is the number of bonds directly involved in the reaction ($n = 5$ for 1,3-dipolar cycloadditions), δB_i is the relative variation of a given Wiberg bond index B_i at the transition state relative to reactants (R), and products (P) and it is calculated as:

$$\delta B_i = \frac{B_i^{TS} - B_i^{R}}{B_i^{P} - B_i^{R}} \quad (8)$$

If the δB_i value is negative it is assumed to be zero. The average value of δB_i (δB_{av}) is defined as:

$$\delta B_{av} = n^{-1} \sum_{i=1}^{n} \delta B_i \quad (9)$$

For ylide $C_5H_5N^+CH^-C(O)Me$, two conformers were calculated (**II** and **IIa**, Table S2 and Table S3), and the first one was found to be the most stable. The activation and reaction energies were estimated relative to **II**.

Acknowledgements

We thank the Federal Targeted Program "Scientific and Scientific-Pedagogical Personnel of the Innovative Russia in 2009–2013" (contract No. P1294 from 09/06/2010), Federal Grant-in-Aid Program "Human Capital for Science and Education in Innovative Russia" for 2009–2013, (agreement No. 14.B37.21.0794 from 03/09/2012), Russian Fund for Basic Research (grants 11-03-00262 and 12-03-33071). We acknowledge Saint Petersburg State University for a research grant (2011–2013) and grant for applied researches (2012–2013), and RAS Presidium Subprogram. A.L.M. expresses his gratitude to the Government of Saint Petersburg for grants for graduate and undergraduate students (2011, 2012). M.L.K. is grateful to the FCT and IST for a research contract within the Ciencia 2007 scientific program. We thank the Computer Center (at Petrodvorets) of Saint Petersburg State University for providing their computer facilities for the theoretical calculations. We are obliged to the FSUE IREA Shared Research Analytic Center (Moscow, Russia) sponsored by the Federal Targeted Program "Research and Development in the Priority Areas for the Development of Scientific and Technological Complex of Russia for 2007–2013" (contract No. 16.552.11.7054 from 12/06/2012) for providing ICP-MS analysis.

Keywords: boranes · cycloaddition · density functional calculations · nucleophilic addition · reaction mechanisms

[1] I. B. Sivaev, V. V. Bregadze, *Eur. J. Inorg. Chem.* **2009**, 1433–1450.
[2] I. B. Sivaev, V. I. Bregadze, N. T. Kuznetsov, *Russ. Chem. Bull.* **2002**, *51*, 1362–1374.
[3] I. B. Sivaev, V. I. Bregadze, S. Sjöberg, *Collect. Czech. Chem. Commun.* **2002**, *67*, 679–727.
[4] I. B. Sivaev, N. A. Votinova, V. I. Bragin, Z. A. Starikova, L. V. Goeva, V. I. Bregadze, S. Sjoberg, *J. Organomet. Chem.* **2002**, *657*, 163–170.
[5] B. Ringstrand, P. Kaszynski, V. G. Young, Z. Janou, *Inorg. Chem.* **2010**, *49*, 1166–1179.
[6] I. N. Polyakova, K. Y. Zhizhin, N. T. Kuznetsov, *Crystallogr. Rep.* **2007**, *52*, 271–274.
[7] G. Froehner, K. Challis, K. Gagnon, T. Getman, R. Luck, *Synthesis and Reactivity in Inorganic, Metal-Organic and Nano-Metal Chemistry* **2006**, *36*, 777–785.
[8] V. Sícha, J. Plesek, M. Kvícalová, I. Císarová, B. Grüner, *Dalton Trans.* **2009**, 851–860.
[9] A. P. Zhdanov, M. V. Lisovsky, L. V. Goeva, G. A. Razgonyaeva, I. N. Polyakova, K. Y. Zhizhin, N. T. Kuznetsov, *Russ. Chem. Bull.* **2009**, *58*, 1694–1700.
[10] A. P. Zhdanov, I. N. Polyakova, G. A. Razgonyaeva, K. Y. Zhizhin, N. T. Kuznetsov, *Russ. J. Inorg. Chem.* **2011**, *56*, 847–855.
[11] A. L. Mindich, N. A. Bokach, F. M. Dolgushin, M. Haukka, L. A. Lisitsyn, A. P. Zhdanov, K. Y. Zhizhin, S. A. Miltsov, N. T. Kuznetsov, V. Y. Kukushkin, *Organometallics* **2012**, *31*, 1716–1724.
[12] N. A. Bokach, *Russ. Chem. Rev.* **2010**, *79*, 89–100.
[13] N. A. Bokach, M. L. Kuznetsov, V. Y. Kukushkin, *Coord. Chem. Rev.* **2011**, *255*, 2946–2967.
[14] V. Y. Kukushkin, A. J. L. Pombeiro, *Chem. Rev.* **2002**, *102*, 1771–1802.
[15] M. L. Kuznetsov, *Russ. Chem. Rev.* **2006**, *75*, 1045–1073.
[16] A. S. Kritchenkov, N. A. Bokach, M. L. Kuznetsov, F. M. Dolgushin, T. Q. Tung, A. P. Molchanov, V. Y. Kukushkin, *Organometallics* **2012**, *31*, 687–699.
[17] A. S. Kritchenkov, N. A. Bokach, M. Haukka, V. Y. Kukushkin, *Dalton Trans.* **2011**, *40*, 4175–4182.
[18] N. A. Bokach, I. A. Balova, M. Haukka, V. Y. Kukushkin, *Organometallics* **2011**, *30*, 595–602.
[19] N. A. Bokach, A. V. Khripoun, V. Y. Kukushkin, *Inorg. Chem.* **2003**, *42*, 896–903.
[20] G. Wagner, M. Haukka, J. J. R. Frausto da Silva, A. J. L. Pombeiro, V. Y. Kukushkin, *Inorg. Chem.* **2001**, *40*, 264–271.
[21] K. V. Luzyanin, A. G. Tskhovrebov, M. F. C. Guedes da Silva, M. Haukka, A. J. L. Pombeiro, V. Y. Kukushkin, *Chem. Eur. J.* **2009**, *15*, 5969–5978.
[22] F. Risitano, G. Grassia, G. Brunob, F. Nicolbb, *Liebigs Ann.* **1997**, 441–445.
[23] W. Zecher, F. Krohnke, *Chem. Ber.* **1961**, *94*, 690–697.
[24] M. F. Aldersley, S. H. Chishti, F. M. Dean, M. E. Douglas, D. S. Ennis, *J. Chem. Soc. Perkin Trans. 1* **1990**, 2163–2174.

[25] O. Tsuge, S. Kanemasa, S. Takenaka, *Bull. Chem. Soc. Jpn.* **1985**, *58*, 3137 – 3157.
[26] O. Tsuge, S. Kanemasa, S. Takenaka, *Bull. Chem. Soc. Jpn.* **1985**, *58*, 3320 – 3336.
[27] I. I. Druta, M. A. Andrei, C. I. Ganj, P. S. Aburel, *Tetrahedron* **1999**, *55*, 13063 – 13070.
[28] G. Matusiak, *Aust. J. Chem.* **1999**, *52*, 149 – 151.
[29] S. Kanemasa, S. Takenaka, H. Watanabe, O. Tsuge, *J. Org. Chem.* **1989**, *54*, 420 – 424.
[30] Y. Shang, M. Zhang, S. Yu, K. Ju, C. Wang, X. He, *Tetrahedron Lett.* **2009**, *50*, 6981 – 6984.
[31] F. Dumitrascu, C. I. Mitan, C. Draghici, M. T. Caproiu, D. Raileanu, *Tetrahedron Lett.* **2001**, *42*, 8379 – 8382.
[32] R. S. Tewari, A. Bajpai, *J. Chem. Eng. Data* **1985**, *30*, 505 – 507.
[33] Y. Kobayashi, I. Kumadaki, E. Kobayashi, *Heterocycles* **1981**, *15*, 1223 – 1225.
[34] R. E. Banks, S. N. Mohialdin, *J. Fluorine Chem.* **1986**, *34*, 275 – 279.
[35] R. E. Banks, S. N. Khaffaff, *J. Fluorine Chem.* **1991**, *51*, 407 – 418.
[36] R. E. Banks, J. Thomson, *J. Chem. Soc. Perkin Trans. 1* **1986**, 1769 – 1776.
[37] J. Alvarez-Builla, E. Galvez, A. M. Cuadro, F. Florencio, S. Garcia-Blanco, *J. Heterocycl. Chem.* **1987**, *24*, 917 – 926.
[38] N. S. Prostakov, V. I. Kuznetsov, G. Dattaray, N. D. Sergeyeva, *Khim. Geterotsikl. Soedin.* **1980**, *6*, 806 – 807. *Chem. Abs.* **1980**, *93*, 168088.
[39] L. Depature, G. Surpateanu, *Spectrochim. Acta Part A* **2003**, *59*, 3029 – 3039.
[40] A. M. Shestopalov, Y. A. Sharanin, V. P. Litvinov, V. N. Nesterov, A. S. Demerkov, V. E. Shklover, Y. T. Struchkov, *Izvestiya Akad. Nauk SSSR Seriya Khim.* **1991**, 697 – 701. *Chem. Abs.* **1991**, *116*, 128606.
[41] K. Dickoré, F. Kröhnke, *Chem. Ber.* **1960**, *93*, 2479 – 2485.
[42] J. Alvarez-Builla, J. L. Novella, E. Gálvez, P. Smith, F. Florencio, S. Garciá-Blanco, J. Bellanato, M. Santos, *Tetrahedron* **1986**, *42*, 699 – 708.
[43] M. Yamazaki, K. Noda, M. Hamana, *Chem. Pharm. Bull.* **1970**, *18*, 901 – 907.
[44] W. Augstein, F. Kroehnke, *Justus Liebigs Ann. Chem.* **1966**, *697*, 158 – 170.
[45] A. M. Shestopalov, Y. A. Sharanin, I. A. Aitov, V. N. Nesterov, V. E. Shklover, Y. T. Struchkov, V. P. Litvinov, *Khim. Geteritsikl. Soedin.* **1991**, 1087 – 1094. *Chem. Abstr.* **1991**, *116*, 214304.
[46] Y. Tominaga, Y. Miyake, H. Fujito, K. Kurata, H. Awaya, Y. Masuda, G. Kobayashi, *Chem. Pharm. Bull.* **1977**, *25*, 1528 – 1533.
[47] C. K. Ghosh, S. Sahana, *Indian J. Chem. Sect. B: Org. Chem. Incl. Med. Chem.* **1996**, *35*, 203 – 206. *Chem. Abs.* **1996**, *124*, 260793.
[48] W. J. Geary, *Coord. Chem. Rev.* **1971**, *7*, 81 – 122.
[49] A. Szwajca, A. Katrusiak, M. Szafran, *J. Mol. Struct.* **2004**, *705*, 159 – 165.
[50] D. Dou, I. J. Mavunkal, J. A. K. Bauer, C. B. Knobler, M. F. Hawthorne, S. G. Shore, *Inorg. Chem.* **1994**, *33*, 6432 – 6434.
[51] F. H. Allen, O. Kennard, D. G. Watson, L. Brammer, A. G. Orpen, R. Taylor, *J. Chem. Soc. Perkin Trans. 2* **1987**, S1 – S19.
[52] J.-C. Zhuo, K. Schenk, *Helvetica Chimica Acta* **1997**, *80*, 2137 – 2147.
[53] M. Basato, B. Corain, M. Cofler, A. C. Veronese, G. Zanotti, *Chem. Commun.* **1984**, 1593 – 1594.
[54] C. O. Kappe, E. Terpetschnig, G. Penn, G. Kollenz, K. Peters, E.-M. Peters, H. G. von Schnering, *Liebigs Ann.* **1995**, 537 – 543.
[55] M. L. Kuznetsov, V. Y. Kukushkin, A. I. Dement'ev, A. J. L. Pombeiro, *J. Phys. Chem. A* **2003**, *107*, 6108 – 6120.
[56] M. L. Kuznetsov, V. Y. Kukushkin, *J. Org. Chem.* **2006**, *71*, 582 – 592.
[57] M. L. Kuznetsov, A. A. Nazarov, L. V. Kozlova, V. Y. Kukushkin, *J. Org. Chem.* **2007**, *72*, 4475 – 4485.
[58] M. L. Kuznetsov, V. Y. Kukushkin, A. J. L. Pombeiro, *J. Org. Chem.* **2010**, *75*, 1474 – 1490.
[59] G. Wagner, A. J. L. Pombeiro, V. Y. Kukushkin, *J. Am. Chem. Soc.* **2000**, *122*, 3106 – 3111.
[60] P. H. H. Hermkens, J. H. von Maarseveen, C. G. Kruse, H. W. Scheeren, *Tetrahedron* **1988**, *44*, 6491 – 6504.
[61] R. Sustmann, *Tetrahedron Lett.* **1971**, *12*, 2717 – 2720.
[62] R. Sustmann, *Tetrahedron Lett.* **1971**, *12*, 2721 – 2724.
[63] A. H. Soloway, W. Tjarks, B. A. Barnum, F. Rong, R. F. Barth, I. M. Codogni, J. G. Wilson, *Chem. Rev.* **1998**, *98*, 1515 – 1562.
[64] L. Zhang, M. Brookhart, P. S. White, *Organometallics* **2006**, *25*, 1868 – 1874.
[65] U. Beckmann, G. Hägele, W. Frank, *Eur. J. Inorg. Chem.* **2010**, 1670 – 1678.
[66] A. F. Lugo (née Gushwa), A. F. Richards, *Eur. J. Inorg. Chem.* **2010**, 2025 – 2035.
[67] M. Basato, E. Caneva, C. Tubaro, A. C. Veronese, *Inorg. Chim. Acta* **2009**, *362*, 2551 – 2555.
[68] L. A. Lesikar, A. F. Gushwa, A. F. Richards, *J. Organomet. Chem.* **2008**, *693*, 3245 – 3255.
[69] K. Y. Zhizhin, V. N. Mustyatsa, E. Y. Matveev, V. V. Drozdova, N. A. Votinova, I. N. Polyakova, N. T. Kuznetsov, *Russ. J. Inorg. Chem.* **2003**, *48*, 671 – 675. *Chem. Abstr.* **2003**, *140*, 77181.
[70] I. Sasaki, L. Vendier, A. Sournia-Saquet, P. G. Lacroix, *Eur. J. Inorg. Chem.* **2006**, 3294 – 3302.
[71] a) V. G. Chekhuta, L. A. Kucherova, *Metody Poluch. Khim. Reakt. Prep.* **1970**, *22*, 40 – 41.
[72] *BrukerAXS, APEX2-Software Suite for Crystallographic Programs*, Bruker AXS, Inc., Madison, WI, USA, **2009**.
[73] G. M. Sheldrick, *Acta Crystallogr.* **2008**, *A64*, 112 – 122.
[74] O. V. Dolomanov, L. J. Bourhis, R. J. Gildea, J. A. K. Howard, H. Puschmann, *J. Appl. Crystallogr.* **2009**, *42*, 339 – 341.
[75] G. M. Sheldrick, *SADABS-Bruker AXS Scaling and Absorption Correction*, Bruker AXS, Inc., Madison, Wisconsin, USA, **2008**.
[76] A. D. Becke, *J. Chem. Phys.* **1993**, *98*, 5648 – 5652.
[77] C. Lee, W. Yang, R. G. Parr, *Phys. Rev. B* **1988**, *37*, 785 – 789.
[78] M. J. Frisch, et al. Gaussian 03, Gaussian Inc., Pittsburgh PA, **2003**. See the Supporting Information of full citation.
[79] C. Gonzalez, H. B. Schlegel, *J. Chem. Phys.* **1991**, *95*, 5853 – 5860.
[80] C. Gonzalez, H. B. Schlegel, *J. Chem. Phys.* **1989**, *90*, 2154 – 2161.
[81] C. Gonzalez, H. B. Schlegel, *J. Phys. Chem.* **1990**, *94*, 5523 – 5527.
[82] J. Tomasi, M. Persico, *Chem. Rev.* **1994**, *94*, 2027 – 2094.
[83] V. Barone, M. Cossi, *J. Phys. Chem. A* **1998**, *102*, 1995 – 2001.
[84] D. H. Wertz, *J. Am. Chem. Soc.* **1980**, *102*, 5316 – 5322.
[85] J. Cooper, T. Ziegler, *Inorg. Chem.* **2002**, *41*, 6614 – 6622.
[86] A. E. Reed, L. A. Curtiss, F. Weinhold, *Chem. Rev.* **1988**, *88*, 899 – 926.
[87] A. Moyano, M. A. Pericàs, E. Valentí, *J. Org. Chem.* **1989**, *54*, 573 – 582.
[88] B. Lecea, A. Adeta, G. Rea, J. M. Ugalde, F. P. Cossío, D. Toma, *J. Am. Chem. Soc.* **1994**, *116*, 9613 – 9619.
[89] I. Morao, B. Lecea, F. P. Cossío, *J. Org. Chem.* **1997**, *62*, 7033 – 7036.
[90] F. P. Cossío, I. Morao, H. Jiao, P. v. R. Schleyer, *J. Am. Chem. Soc.* **1999**, *121*, 6737 – 6746.

Received: September 27, 2012
Published online on November 23, 2012

